The 2010 IEEE/RSJ International Conference on
Intelligent Robots and Systems
October 18-22, 2010, Taipei, Taiwan

Development of a Child-Oriented Social Robot for Safe and Interactive Physical Interaction

Xiaoning Ma and Francis Quek

Abstract— **As an important approach to ensure safety and naturalness, compliant motion is already implemented in large-size robots, but it is still an undeveloped area in child-oriented robots as it calls for a lightweight and compact solution compared with large-size robots. In this paper, we proposed the design of a social robot which aims at conducting safe and playful Human-Robot Interaction (HRI), especially with children. We built a teddy bear robot prototype based on hybrid passive-active compliant system which consists of flexible joints as passive part and compliant motion controller as active part. The compliant controller detects external perturbation through motor state variables, therefore force and torque sensors could be omitted to keep overall system compact. Experiments conducted in typical HRI scenarios showed that the hybrid passive-active compliant system enabled our robot to conduct safer and more interactive physical interaction compared with robot under traditional control method.**

I. INTRODUCTION

Child-oriented robot, as an important branch of social robot, has drawn considerable and increasing attention in the past few years [1]. The new trend of social robotics research and application in the context of children care, education and entertainment calls for a lightweight, compact and cost-effective solution to address many issues in the advance toward better Human-Robot Interaction (HRI). Among these issues, the ability to conduct safe and natural physical contact, and thereby allow playful physical interaction with children in a uncertain and unpredictable environment [2] [3] becomes one of the key issues.

In the field of large scale robots, compliant motion control has been widely adopted in multi-link manipulators [4] and human-sized robots [5] [6]. Compared to small scale personal robots, large scale robots usually emphasize precision and response speed of motion control [7] rather than size, weight and power consumption, therefore it is acceptable to use torque sensor, complex mechanism and computationally intense algorithm to control multi-link manipulators. In contrast, small scale robots usually require to reduce system size, weight and power consumption, as well as lower the complexity of mechanical design and control method to achieve fast response speed and natural motion. Recently, many attempts have been made to use Series Elastic Actuator (SEA) to introduce intrinsic compliance into robotic systems [8] [9], and some of them aim at ultilizing SEA in small scale robots, such as [10]. While these works sought to address the safety issue from a methodological perspective by proposing SEA structure and control strategy design, and conducting analytical unit-level evaluation, our work proposes a light-weight and compact integrated design which balances between system constraints and compliance performance, as well as an evaluation of overall robot system performance from the point of user's perception towards the physical contact.

In this paper, we developed an autonomous teddy bear social robot as an embodiment of compliant physical motion and a platform to study the impact of interactive playfulness in human-robot interaction, especially interaction with children. The contribution of the paper lies in:

(i) An integrated system design for compliant motion in child-oriented social robot is proposed. The design enables the robot to intuitively comply to perturbation as well as maintaining its own autonomy. The controller operates in absence of sensory information from torque or force sensor, thereby reduces the complexity of mechanism and overall system cost.

(ii) The mechanical design of a compact and lightweight flexible joint and its physical model is proposed, which provides instant compliance and especially fulfills the system requirements of small-size robot.

(iii) Experiments in different scenarios during physical Human-Robot Interaction (pHRI) is conducted, and proved that compared with conventional controlled robot, our robot could perform better in conducting physically safe and interactive contact.

II. METHODOLOGY

A. Analysis of Physical Human-Robot Interaction

A sketch diagram of the physical contact between human and robot is demonstrated in Fig. 1. In the diagram, robot's joint is driven by the actuator, and is also deflected by the external influence from human in the same time. Here the actuating torque Γ_{act} is set by actuator controller, hence the rotary torque of rotor and physical joint, Γ_{rot} and Γ_{jnt} are observable, whereas the torque imposed by human, Γ_{ext}, is unpredictable and unobservable provided when no torque and force sensing device is equipped in the robot. Γ_{ext} also represents the impact imposed on human, therefore keeping Γ_{ext} in a safe and natural range would be desirable to provide sense of liveness to human during pHRI.

This work was done when Xiaoning Ma was with Social Robotics Laboratory, Interactive and Digital Institute, National University of Singapore. Email: xiaoning84@gmail.com

Fransic Quek is with Vision Interfaces and Systems Laboratory, Center for Human Computer Interaction, Virginia Polytechnic Institute and State University, Blacksburg, VA 24060, USA. Email: quek@vt.edu

978-1-4244-6676-4/10/$25.00 ©2010 IEEE

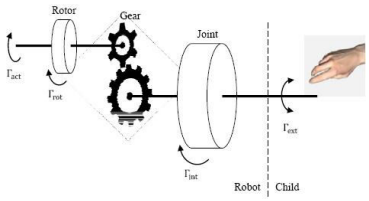

Fig. 1. A sketch diagram of physical Human-Robot Interaction.

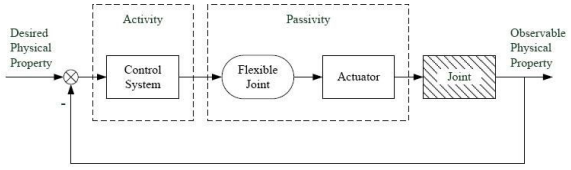

Fig. 2. Diagram of hybrid passive-active compliant motion control system.

Given the gear ratio in Fig. 1 is denoted by N, the torque balance between both sides can be represented as follow:

$$\Gamma_{act} = \Gamma_{rot} + \frac{\Gamma_{jnt}}{N} + \frac{\Gamma_{ext}}{N} \tag{1}$$

In many common pHRI scenarios, human would actively influence the robot side and consequently break this balance. Based on Equation (1), this condition can be expressed as follow (Γ_{rot} is neglected since it is normally omissible compared with Γ_{act} and Γ_{jnt}):

$$\Gamma_{ext} > N\Gamma_{act} - \Gamma_{jnt} \tag{2}$$

Equation (2) showed that robots would not comply with human unless Γ_{ext}, the torque imposed by human, exceeds $N\Gamma_{act}$. Since that output torque of most commonly used motors is far beyond the normal range of human's influence on robot, conventional stiff-controlled robots will behave as a rigid machine without any intelligent compliance, which might lead to unpleasant user experience and underlying danger of injury to human.

B. Solution to the Problem

One solution of the problem is to adjust Γ_{act} in accordance with Γ_{ext}, which will change the Equation (1) into the equation below:

$$\Gamma_{act}(\Gamma_{ext}) = \frac{\Gamma_{jnt}}{N} + \frac{\Gamma_{ext}}{N} \tag{3}$$

In most applications Γ_{ext} is obtained in real-time from torque sensors, which is widely used in large scale robots and manipulators such as DLR-III lightweight robot [11] and Honda [6]. In small scale child-oriented robots, limitations on size, weight and power consumption are more strict, hence a cost-effective and power-efficient system design with less sensory devices applied will be the most desirable.

For any robotics application, design of actuator system, sensory system, mechanism and control scheme need to be considered as an integrated solution to address the hypothesis embodied in this application [12], and the balance between performance and other issues including safety and system cost needs to be achieved [13]. In small-size robot, DC micro motors are the most frequently used actuators since they could provide wide range of torque and speed in small size (which also highlights the necessity and importance of compliance feature in child-oriented robots). In mechanical design, elastic components could be utilized to compensate the reaction delay of control system as the computing system integrated in small-size robots might not be high-performance due to system constraints. With the elasticity introduced by flexible joint and the electromagnetic property of actuator, mechanical system and actuator system could reflect external perturbation through physical signals, which would be detected and computed by control system, thus it is possible to implement information sensing in control system instead of an independent sensory system, thereby keep the whole system compact and cost-effective. In this design, the control system would enable the robot to actively follow human's interaction force, while the flexible joint could provide passivity for instant reaction to external perturbation. This passive-active hybrid system can be demonstrated in Fig. 2.

As position control is the most frequently used control scheme in robotics applications, it is possible to use joint position as one of the physical signals to reflect external perturbation. The hardness of elastic components is another element which affects the external perturbation. Both elements will take effect on the position control system, and the effect could be observed through actuator position and armature current, which are both measurable in actuator system. With this design approach, the pHRI process presented in Equation (3) can be further extended as follow:

$$N \cdot \Gamma_{act}(\theta_{act}, i_{act}) = \Gamma_{jnt}(\ddot{\theta}_{jnt}, \theta_{jnt}) + \Gamma_{ext}(\theta_{act}, \theta_{jnt}, k) \tag{4}$$

where θ_{act} and θ_{jnt} denote the position of actuator and physical joint, i_{act} denotes the current of motor, and k denotes the coefficient of the elastic component in flexible joint.

Following this design principle, we developed a child-oriented, fully autonomous teddy bear social robot which aims at conducting natural and playful physical interaction with children, as is shown in Fig. 3. Three typical scenarios are also described in Fig. 3. In the first scenario, a child is using his hand to stop the movement of robot's arm. In this case, cooperatively stopping pushing against the child would give a sense of naturalness and liveliness. In the second scenario, a child and a robot are holding each other's hands and swinging their arms back and forth. In this case, the robot would give the child a sense of naturalness and liveliness if it could spontaneously follow the child's action. In the third scenario which a child suddenly pushed robot on one of its joints, a quick withdrawal would not only make the robot's behavior more life-like, but also ensure safety for both child and robot.

Fig. 3. The picture of our teddy bear social robot which is built based on the hybrid passive-active compliant motion system and aims at playing with children physically with a sense of interactivity and naturalness. The figures below demonstrated how the robot could cope with children's unpredictable behavior with the effect of hybrid compliant motion system.

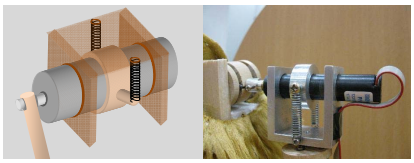

Fig. 4. Design drawing and picture of 1-DOF flexible joint.

As an implementation of this design principle, the robot is designed to have a lovely bear-like appearance with furry exterior and cotton filled inside. It has three 1-DOF flexible joints: one for neck and two for shoulders. Each joint is built with a DC motor and a flexible joint, and the motor is controlled by a compliant motion controller. Extra sensor equipments (torque, force sensor, potential meter, etc.) are excluded to ensure system simplicity and efficiency, which also means the sensory information of control algorithm is limited to actuator system data only.

III. PASSIVE COMPLIANT MECHANISM

Following the conception stated in former chapters, we designed and developed a flexible joint with elastic mechanism to support passive instant compliant reaction. Besides, simple structure, low weight and low cost also allow it to be utilized in small-size robots. As is shown in Fig. 4, a pair of spiral springs are mounted between the frame and motor shell to provide compliance to external force. Both springs are identical and pre-stretched to the same length.

The physical model of the design in Fig. 4 can be illustrated as a dual spring-lever system as shown in Fig. 5. Given that the original length of both springs is L_0 and the pre-stretched length is $L(L > L_0)$, the linear elastic coefficient of both springs is k', the vertical distance between the mount point on the levers and the axis of motor is R, when the motor rotates against the bracket at an angle of $\Delta\theta$ and results in the lengths of springs becoming $L_1(L_1 > L)$ and $L_2(L > L_2 > L_0)$, the torque applied to make the $\Delta\theta$'s rotation can be computed as follow (the horizontal displacement of both mount points on the levers during the rotation is omitted):

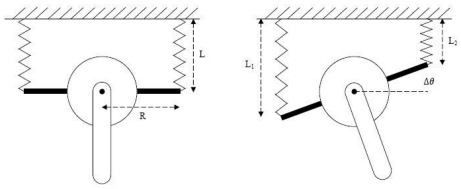

Fig. 5. The physical model of flexible joint can be represented as a dual lever-spring system, with two identical spiral springs mounted between the motor bracket which is attached on the frame of robot and two levers which are fixed on motor shell.

TABLE I

PHYSICAL PARAMETERS OF FLEXIBLE JOINT

Parameter	Value
m_a	0.147kg
L_a	0.14m
k'	490N/m
R	0.012m

$$\begin{aligned}\Gamma = \Gamma_1 - \Gamma_2 &= k'R(L_1 - L_2)\cos\Delta\theta \\ &= k'R^2\sin(2\Delta\theta) \end{aligned} \quad (5)$$

Then the equivalent torsional elastic coefficient k can be obtained as follow:

$$k = \frac{\Gamma}{\Delta\theta} = \frac{k'R^2}{\Delta\theta}\sin(2\Delta\theta) \quad (6)$$

The physical parameters of the flexible joint showed in Fig. 4 are listed in Table I (m_a and L_a represent the weight and length of the load that mounted on motor shaft, respectively). These parameters are selected through repetitive tests with the purpose of both minimizing the error introduced by elasticity and ensuring small size and light weight.

IV. ACTIVE COMPLIANT CONTROLLER

Fig. 6 showed the block diagram of the whole compliant motion controller which in based on position control system. Give that FP denotes the transform function of the forward path of position loop and velocity loop, and CL denotes the transform function of closed current loop, then the output torque of actuator can be computed as follow,

$$\Gamma_{act} = K_e \cdot FP \cdot CL \cdot (\theta_{cmd} - \theta_{act}) \quad (7)$$

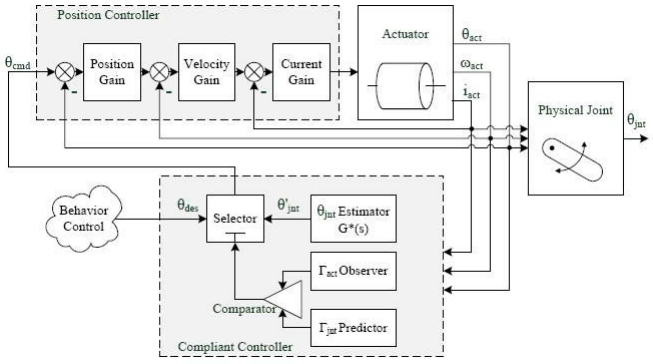

Fig. 6. The framework of compliant motion control system.

When there is no displacement in dual spring-lever system, the the rotary torque of physical joint can be observed by the position of actuator as follow,

$$\Gamma_{jnt} = J\ddot{\theta}_{act} + \Gamma_{gvt}\sin\theta_{act} \tag{8}$$

where Γ_{gvt} denotes the maximum gravity torque of the physical joint. When displacement occurs in the dual spring-lever system and results in the difference between θ_{jnt} and θ_{act}, Equation (8) is modified as follow,

$$\Gamma_{jnt} = J\ddot{\theta}_{act} + \Gamma_{gvt}\sin\theta_{jnt} \tag{9}$$

External perturbation is not directly observable, but can be represented as in Equation (5). By substituting Equation (5), (7) and (9) into Equation (4), we can obtain the implementation of this physical contact model on the basis of motor position control:

$$\begin{aligned} &N\cdot K_e\cdot FP\cdot CL\cdot(\theta_{cmd}-\theta_{act}) = \\ &\quad J\ddot{\theta}_{act} + \Gamma_{gvt}\sin\theta_{jnt} + k'R^2\sin 2(\theta_{jnt}-\theta_{act}) \end{aligned} \tag{10}$$

It is obvious to see that one of the effective ways to achieve natural and compliant physical interaction is to keep Γ_{ext} in a relatively low range by controlling θ_{act} to follow up the unpredictable variation of θ_{jnt}, which can be realized by sending position command θ_{cmd} to the input of three closed-loop controller, as demonstrated in Fig. 6 and in the left side of Equation (10). In order to identify the transform function of the transform unit in Fig. 6, we can use observable processes as substitution of the control law in the left side of Equation (10), thereby to simplify the computation of solving θ_{jnt}:

$$NK_e i_{act} = J\ddot{\theta}_{act} + \Gamma_{gvt}\sin\theta_{jnt} + k'R^2\sin 2(\theta_{jnt}-\theta_{act}) \tag{11}$$

By applying Taylor Series into Equation (11) and considering the mechanical and design limitation on θ_{jnt} and θ_{act}, the trigonometric functions in Equation (11) can be extended as follow,

$$\begin{cases} \sin\theta_{jnt} = \theta_{jnt} + \Delta_{\varepsilon 1} \\ \Delta_{\varepsilon 1} = \displaystyle\sum_{k=3}^{\infty}(-1)^k\frac{\theta_{jnt}^k}{k!} \qquad (|\theta_{jnt}| \le \frac{\pi}{3}) \end{cases} \tag{12}$$

$$\begin{cases} \sin 2(\theta_{jnt}-\theta_{act}) = 2(\theta_{jnt}-\theta_{act}) + \Delta_{\varepsilon 2} \\ \Delta_{\varepsilon 2} = \displaystyle\sum_{k=3}^{\infty}(-1)^k\frac{2^k(\theta_{jnt}-\theta_{act})^k}{k!} \\ \qquad\qquad (|\theta_{jnt}-\theta_{act}| \le \frac{\pi}{6}) \end{cases} \tag{13}$$

Hence Equation (11) can be simplified by substituting Taylor Series expansion above into trigonometric functions as follow,

$$NK_e i_{act} = J\ddot{\theta}_{act} + \Gamma_{gvt}\theta'_{jnt} + 2k'R^2(\theta'_{jnt}-\theta_{act}) \tag{14}$$

Here θ'_{jnt} denotes the approximation of actual θ_{jnt} as Equation (11) is simplified as approximated by applying Taylor Series. Equation (14) is an approximation of the original pHRI model expressed in Equation (10), as three and higher order terms in Taylor Series extension of trigonometric functions are omitted in Equation (14). According to the angle limitations from mechanical design and software implementation, the error of Equation (14) can be further computed as follow,

$$\begin{aligned} \Delta_{\varepsilon 1} &< \left|(-1)^k\frac{\theta_{jnt}^k}{k!}\right|\Bigg|_{k=3,\theta_{jnt}=\frac{\pi}{3}} \\ &\approx 0.191 \end{aligned} \tag{15}$$

$$\begin{aligned} \Delta_{\varepsilon 2} &< \left|(-1)^k\frac{2^k(\theta_{jnt}-\theta_{act})^k}{k!}\right|\Bigg|_{k=3,\theta_{jnt}=\frac{\pi}{3},\theta_{act}=\frac{\pi}{6}} \\ &\approx 0.192 \end{aligned} \tag{16}$$

Based on the selected parameters listed in Table I, the error of Equation (14) introduced by Taylor Series extension can be computed as

$$\Delta_{\varepsilon} = \Gamma_{gvt}\Delta_{\varepsilon 1} + 2k'R^2\Delta_{\varepsilon 2} \approx 0.046Nm \tag{17}$$

which is negligible compared with the output torque of the motors selected in our prototype, which normally generate over $1Nm$'s torque when physical impact is happening. Therefore, the transform unit $G^*(s)$ in Fig. 6 can be defined from Equation (14) as follow,

$$\theta_{fwd} = \theta'_{jnt} = \frac{2kR^2\theta_{act} - J\dot{\omega}_{act} + NK_e i_{act}}{\Gamma_{gvt} + 2kR^2} \tag{18}$$

The condition that determines whether the feed forward position command is taking effect is defined by

$$\begin{cases} N\Gamma_{act} = \Gamma_{jnt} & \text{(Condition of Autonomy)} \\ N\Gamma_{act} > \Gamma_{jnt} & \text{(Condition of Compliance)} \end{cases} \tag{19}$$

When the compliance condition is satisfied, the transform unit in Fig. 6 is taking effect, the position command θ_{cmd} would be set to zero to temporarily cancel the effect of position control from higher level software, thereby allow autonomy and compliance to coexist in one system and switch back and forth in accordance with external condition as an intelligent creature.

V. EXPERIMENT RESULTS

Experiments were conducted to verify the performance of the robot's compliant motion. Three typical pHRI scenarios as discussed in Section II were analyzed in the experiments. Three different test prototypes are used in the experiment to show the differences of their performance in pHRI scenarios. The first test prototype is a traditional robotic arm without any compliant feature. The second test prototype is a stiff robotic joint controlled by an active compliant controller, which will be referred to as half-compliant prototype. The Last prototype is our teddy bear robot, which is built with fully-compliant joints that are controlled by hybrid passive-active compliant system. These prototypes are constructed with the same structure and motors, the only difference is

whether active or passive compliance is implemented. We attached a force sensor in the end of robotic arm to detect the force applied by human, so that the torque applied by human Γ_{hmn} can be obtained. The parameters applied in the following experiments are illustrated in Table I in Section III. In the following figures, data from noncompliant prototype is given by blue lines, data from half-compliant and fully-compliant prototype are given by purple and red lines respectively.

A. Motion Blocked

This experiment aims at verifying the improvement of safety and naturalness of physical contact brought by hybrid compliant system. In each case of this experiment, the robot was commanded to raise its arm at the same speed, and the human tester put his hand in front of the arm to stop the motion. Data gathered from force sensor are converted into torque and is shown in Fig. 7, and the experimental result can be obtained as in Table II.

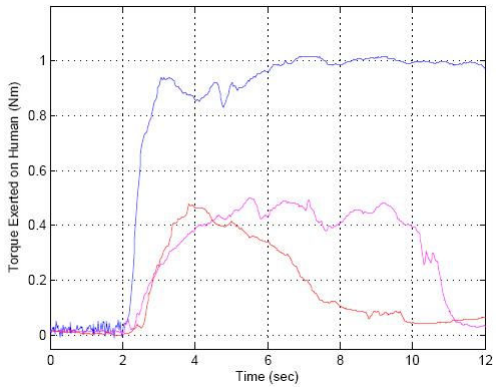

Fig. 7. Torque data gathered from motion-blocked experiment.

TABLE II
RESULT OF MOTION-BLOCKED EXPERIMENT

Data	Stiff	Half-Compliant	Fully-Compliant
Rising Edge Slope (Nm/s)	0.871	0.139	0.253
Torque Peak (Nm)	1.016	0.499	0.477
Impact Duration (s)	∞	9.851	7.906

The experimental result in Table II can be analyzed and summarized as follow.

(i) The torque exerted by stiff robotic arm rose up with a slope of $0.871Nm/s$, then retained at $1.016Nm$ throughout physical impact, which are 3.4 times and 2.1 times higher than the slope and peak value on fully compliant robot joint. This revealed that the torque exerted on children by stiff-controlled robot might be unexpected, fiercely increasing and persistent.

(ii) The duration of physical impact on fully-compliant joint is approximately 2 seconds shorter than the half-compliant joint, which is because the active compliant controller relies on the armature current observation only, which normally takes several seconds to react to the external interference. Passive mechanism can provide instant and structural compliance which could complement active compliance to achieve better performance and life-like characteristics.

B. Arm Sway

This experiment is to examine whether the bear robot could perform better in interactive and playful physical contact with the aid of hybrid compliant system. In this experiment, robot kept still until the tester caught both its hands and swayed its arms back and forth. The displacement of motor (denoted as θ_{act} in former sections) was measured instead of the displacement of joint (denoted as θ_{jnt} in former sections), as no angle sensor was utilized in this experiment. The experimental result is shown and summarized in Fig. 8 and Table III.

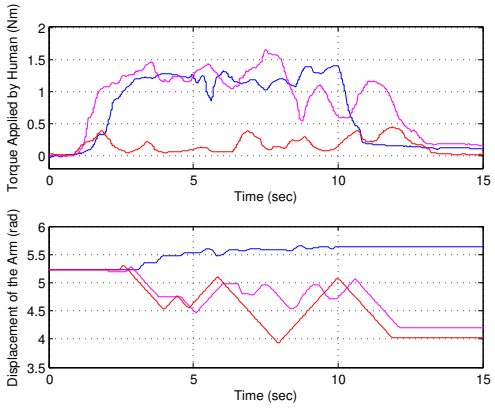

Fig. 8. Torque and motor position data gathered from arm sway experiment.

TABLE III
RESULT OF ARM SWAY EXPERIMENT

Data	Stiff	Half-Compliant	Fully-Compliant
Averaged Torque (Nm)	1.124	0.990	0.173
Position Displacement Range (rad)	0.129	0.593	1.168

Results showed that this stiff-controlled robot could not instinctively follow children's physical interaction. Both half and fully compliant robots are able to follow, and fully compliant robot can provide 2 times wider position displacement range with 82.5% lower average torque applied, compared with half compliant robot, which proved that our compliant bear robot is able to generate more responsive and cooperative behaviors.

C. Fierce Shove

This experiment is to verify whether the bear robot's instinctive compliance could make it more safe to both children and itself when fierce collision happens. In the experiment,

human tester pushed hard on the robot's head along the direction that it was turning slowly. In the three cases of this experiment, human tester pushed the robot's head in approximately the same direction, strength and duration. The experimental data and results are shown in Fig. 9 and Table IV.

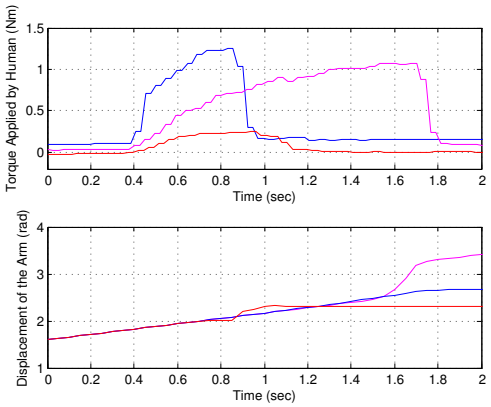

Fig. 9. Torque and motor position data gathered from yank experiment.

TABLE IV
RESULT OF FIERCE SHOVE EXPERIMENT

Data	Stiff	Half-Compliant	Fully-Compliant
Torque Peak (Nm)	1.258	1.076	0.247
Impact Duration (s)	0.589	1.438	1.058
Position Displacement Range (rad)	0	0.756	0.323

From the data shown above, it can be summarized that:

(i) Tester's shove on stiff robot would generate the most fierce and sharp torque to both human and robot. Torque generated from half-compliant robot is relatively milder and lower, and that from fully-compliant robot is 80.4% lower, but $0.469s$ longer than that on stiff robot, which showed that the collision impact was largely lowered by fully-compliant robot.

(ii) Half-compliant robot turned its head to follow the shove but time delay reached $1.2s$. The displacement of motor position on fully-compliant robot is even negligible because effect was mainly absorbed by passive compliance mechanism. However, as presented in Section III, the position displacement provided by flexible joint is limited, and might reach its limitation during severe shock, therefore is also risky in damaging the robot.

VI. CONCLUSIONS AND FUTURE WORK

This paper presented a teddy bear social robot, which is designed to conduct natural and playful physical interaction with children. Our robot demonstrated one of the viable solutions of making social robots physically safe, interactive and playful, and also keep the overall design compact and cost-effective. The proposed design of hybrid compliant motion system in the paper can also be extended into more complicated systems (i.e. multi-DOF system) and more robotics application area (i.e. service robot for elderly and disabled). The design proposed in this paper is experimentally evaluated and the experimental scenarios can also be extended into common scenarios happened during pHRI.

Future research will include a more compact and durable multi-DOF system design to better address children's needs for a playful robot, and a more precise modeling of the hybrid compliant motion system. Future work will also attempt to explore the social impact of compliant behavior on children, and obtain design guidelines that aim at achieving more interactive and playful behavior of child-oriented social robots.

VII. ACKNOWLEDGMENT

The authors would like to thank Prof. Shuzhi Sam Ge for his support and advice for this research, and the reviewers for their valuable feedback.

REFERENCES

[1] T. Fong, I. Nourbakhsh, and K. Dautenhahn, "A survey of socially interactive robots," *Robotics and Autonomous Systems*, vol. 42, pp. 143–166, 2003.

[2] S. Schaal, "The new robotics - towards human-centered machines," *HFSP Journal*, vol. 1, no. 2, pp. 115–126, 2007.

[3] E. Garcia, M. A. Jimenez, P. G. D. Santos, and M. Armada, "The evolution of robotics research," *IEEE Robotics and Automation Magazine*, vol. 14, no. 1, pp. 90–103, 2007.

[4] A. Schneider, H. Cruse, and J. Schmitz, "A biologically inspired active compliant joint using local positive velocity feedback (lpvf)," *IEEE Transactions on Systems, Man and Cybernetics - Part B: Cybernetics*, vol. 35, no. 6, pp. 1120–1130, 2005.

[5] C. Ott, O. Eiberger, W. Friedl, B. Bauml, U. Hillenbrand, C. Borst, A. Albu-Schaffer, B. Brunner, H. Hirschmuller, S. Kielhofer, R. Konietschke, M. Suppa, T. Wimbock, F. Zacharias, and G. Hirzinger, "A humanoid two-arm system for dexterous manipulation," in *Proceedings of the IEEE-RAS International Conference on Humanoid Robots*, pp. 276–283, 2006.

[6] T. Yoshikawa and O. Khatib, "Compliant humanoid robot control by the torque transformer," in *Proceedings of the IEEE/RSJ International Conference on Intelligent Robots and Systems*, pp. 3011–3018, 2009.

[7] C. Ott, A. Albu-Schaffer, A. Kugi, and G. Hirzinger, "On the passivity-based impedance control of flexible joint robots," *IEEE Transactions on Robotics*, vol. 24, no. 2, pp. 416–429, 2008.

[8] R. Schiavi, G. Grioli, S. Sen, and A. Bicchi, "Vsa-ii: a novel prototype of variable stiffness actuator for safe and performing robots interacting with humans," in *Proceedings of IEEE International Conference on Robotics and Automation*, pp. 2171–2176, 2008.

[9] M. Zinn, B. Roth, O. Khatib, and J. K. Salisbury, "A new actuation approach for human friendly robot design,"

[10] N.G.Tsagarakis, M. Laffranchi, B. Vanderborght, and D.G.Caldwell, "A compact soft actuator unit for small scale human friendly robots," in *Proceedings of IEEE International Conference on Robotics and Automation*, pp. 4356–4362, 2009.

[11] G. Hirzinger, A. Albu-Schaffer, M. Hahnle, I. Schaefer, and N. Sporer, "On a new generation of torque controlled light-weight robots," in *Proceedings of the IEEE International Conference on Robotics and Automation*, pp. 3356–3363, 2001.

[12] A. D. Santis, B. Siciliano, A. D. Luca, and A. Bicchi, "An atlas of physical humancrobot interaction," *Mechanism and Machine Theory*, vol. 43, pp. 253–270, 2008.

[13] A. Bicchi, M. Bavaro, and G. Boccadamo, "Physical human-robot interaction: Dependability, safety and performance," in *Proceedings of International Workshop on Advanced Motion Control*, pp. 9–14, 2008.